Hydraulic gas compressor: a low energy intensive and low cost option for CO_2 capture

Valeria Pavese[a], Dean Millar[b] and Vittorio Verda[c]

[a] Mining Innovation, Rehabilitation & Applied Research Corporation (MIRARCO), Sudbury (ON), Canada and Department of Energy (DENERG), Politecnico di Torino, Torino, Italy
vpavese@mirarco.org
[b] MIRARCO, Sudbury, Canada, dmillar@mirarco.org
[c] DENERG, Politecnico di Torino, Torino, Italy, vittorio.verda@polito.it

Abstract:

Hydraulic air compressor (HAC) technology, historically used in the mining industry for compressed air production, is considered for re-engineering as a carbon dioxide separation method. The scheme involves a pressure swing absorption process, engineered by exploiting i) gas dissolution into the liquid at high pressure ii) physical gas-liquid separation and iii) the gas evolution from the separated liquid at low pressure. The solubility of CO_2 in water is approximately one order of magnitude higher than that of N_2, and as gas solubility increases with increasing pressure, this makes HACs of interest in CO_2 capture applications. An exemplar mass, energy and exergy analysis of a HAC with a 40 MW_e natural gas combined cycle gas turbine (CCGT) suggests i) energy penalties below 10%, ii) CO_2 recovery from the flue gas stream over 90% and iii) cost of CO_2 avoided below 50 USD per tonne, with this post-combustion capture technology.

Keywords:

Carbon dioxide capture, Hydraulic air compressor, Pressure swing absorption, Exergy.

1 Introduction

Millar [1] recently reviewed the case for revisiting hydraulic air compressor (HAC) technology for modern air compression tasks, and has noted that, providing the role of gas solubility in water is fully appreciated, there is no reason that this traditional air compression technology may not be used to compress other gases and gas mixtures too. For gases other than air, the technology would be referred to as a hydraulic gas compressor (HGC). This paper explores the use of HACs in a new application area, that of: post-combustion carbon capture. This introduction section outlines the HAC/HGC process and the defining characteristics of the technology. It then sets out the currently leading post-combustion CO_2 technologies. The second section of the paper integrates these aspects to consider the new application proposal starting with motivation and culminating in presentation of process flow calculations for an illustrative example involving a natural gas fired 40 MW_e combine cycle gas turbine (CCGT). This scale of power plant was chosen because it matches the capacity of the largest HAC ever built: Ragged Chutes, located in Cobalt, Northern Ontario which produced ~68,000 Sm^3/h (~40,000 Scfm) compressed air at ~8.3 bar gauge (120 psi) and which operated continuously for around 60 years. It has also been studied extensively, including having been subjected to a formal construction estimation process by an experienced, large scale, multinational construction contractor. Consequently there is high confidence in the capital costs that feed into the techno-economic analysis of Section 3 of the paper. Section 4 presents the results of an exergy analysis of the system to highlight where the major irreversibilities arise, and the final section concludes.

1.1. The hydraulic gas compression process

A hydraulic air compressor may be described as maximally efficient low head – high flow rate (typically of order 10 metres and of order 100 m^3/s) hydropower to pneumatic power conversion devices [2].

In HACs, an air-water atmospheric mixing head is connected to a downward shaft (i.e. the downcomer) which leads to a physical separator device at depth. After the initial mixing process, if the velocity of the water is sufficient for drag forces to overcome buoyancy forces acting on the entrained bubbles, a two-phase bubbly flow is produced. As the fluid flows downward in the downcomer, hydropower is consumed to overcome i) frictional forces, ii) drag and buoyancy forces, iii) other irreversibilities and to compress gas bubbles. At the end of the compression process in the downcomer, a high pressure separation process isolates the compressed gas. Separation can be achieved in a separation gallery: an enlargement of the flow cross-section reduces fluid velocity to permit buoyancy forces acting on the bubbles to prevail over drag to lift gas the bubbles from the water to form a compressed air plenum. This is a gravity separation process but separation could also be performed using cyclonic separators. The latter are more compact, but will introduce greater irreversibility, so are better suited to situations where higher head is available, but HACs are still essentially low head-high flow rate devices. After the separation stage the high pressure air is collected in a delivery pipe and the water passes into a riser shaft to restore the water pressure to the atmospheric value. The difference in elevation between the inlet and outlet location of the water flow represents the driving head of the system.

1.2. Defining characteristics of hydraulic gas compression

The main features characterizing the HGC compression process are:

- Nearly isothermal process: due to the direct contact of the liquid and gas in the downcomer, as the gas phase is compressed the heat developed is simultaneously transferred to the water which provides a natural cooling effect. The liquid phase has mass flow and heat capacity of the order of 1000 and 4 times greater, respectively, than that of the air and for this reason the increment of temperature is on the order of 0.1 K [1].
- Minimum work compression: the compression process approaches an isothermal compression that is the most energy efficient type of process since it required lower specific work in comparison to polytropic and adiabatic processes typical of conventional compressors [2].
- Dissolution of gas phase into the liquid phase: the direct contact of air and water has the disadvantage of permitting the gas species to dissolve in the water. As the pressure increases, gases become more soluble in the water and during the HAC compression a portion of the inlet gas flow rate by-passes the separation stage, since it is dissolved in the liquid phase, and cannot be collected at the delivery point. The solubility losses greatly affect the mechanical efficiency of the system, which can be reduced by up to 30 percent [3].
- Release of the dissolved gases: the part of gases dissolved in the water during the compression comes out of solution as the pressure reaches the atmospheric value once again while the water rises in the riser shaft. This may create an air lift effect for the water that may reduce the input hydropower required to operate the HAC [4].

1.3. State-of-the-art post combustion carbon capture technologies

From the most recent reviews on post-combustion carbon capture system is clear that the most mature technology remains amine-absorption (AA) [5, 6]. The AA process takes place in an absorption column in which the amine solvent is in direct contact with the flue gas and preferentially absorbs the CO_2 present in the gaseous mixture. However, there is no manipulation of pressure to enhance the absorption process. AA requires a regeneration step where the solvent is heated so that the CO_2 is evolved [7]. The main drawback of AA technology is the large amount of heat required in the regeneration step. Most commonly this is provided in the form of steam extracted from the power plant to which the carbon capture system is retrofitted. Amine degradation, which results in solvent loss and leads to equipment corrosion, is also a major concern and the flue gas requires cooling and treatment before entering the absorption column [7, 8]. These aspects may mean that despite its promise, AA may not be the final CO_2 capture system of choice.

Table 1. Comparison of main parameters defining mature or nearly mature post-combustion capture technologies

Method	Type	Temp. (°C)	Pres. (bar)	Carrying capacity	CO_2 removal efficiency (%)	Purity (wt.%)	Energy consumption	Estimated cost
Chemical absorption	MEA 30 wt.% [12]	40 – 120	1	0.409 $kgCO_2/kgMEA$	89 – 96 [13]	99 – 99.2	0.97 – 4.2 GJ/tCO_2 [5, 13, 14]	30 – 91 $US\$/tCO_2$ captured [15]
	Ammonia [9]	<20	1	1.2 $kgCO_2/kgNH_3$	99 [12]	99.9	2.8 GJ/tCO_2 [5]	41 – 69 $US\$/tCO_2$ captured [15]
Solid adsorption	Calcium looping [10]	>600	1	NA	90	> 99.9	Energy penalty of 7 – 8%	29 – 50 $US\$/tCO_2$ avoided
	Activated carbon [9]	25 – 75	1	0.003–0.154 $kgCO_2/kgAC$	90	> 95 [11]	0.7 – 0.8 GJ/tCO_2	NA
Membrane	Polymeric [8]	100	15 – 20	NA	90	> 95	0.5 – 6 GJ/tCO_2 [8] Energy penalty of 16-30% for VSA [11]	25 – 40 $US\$/tCO_2$ avoided [11]

Thus alternatives to AA are under development for post-combustion capture, such as ammonia absorption [9], chemical looping combustion [10] or membrane separation [8]. Entries 1 to 5 of Table 1 report the characterizing parameters of competing processes that have reached a technology readiness level of 5 [11] or higher and have thus been validated in relevant environment.

2. Application of HGC to carbon capture

In comparison to the leading chemical absorption CO_2 capture technologies, HAC technology offers several advantages:

- No need for a separate flue-gas pre-cooling stage before the separation process. As reported in Table 1 the temperature of the flue gas, typically above 100°C, has to be reduced before entering the absorption column in order to facilitate the absorption process or to meet the limit of volatility of the solvent used (as in the ammonia process) [9, 16]. In a HGC the cooling effect is provided directly by entraining water flowing.
- No need for steam draw-off from the steam turbine in plants featuring a Rankine cycle. In the chemical absorption processes, the heat required to feed the reboiler of the regenerator is supplied in the form of 'parasitic' steam from the power station. In a HGC, 'regeneration' results from depressurization in the riser.
- No need for exhaust condensate return from the capture plant to the power plant: the steam once condensed has to be returned to the power plant.

- No need for a distinct water removal stage during CO_2 compression in transportation and storage stages. A dry stream of gas is produced from a HGC due to low saturation vapour pressure at pressure and integrated physical separation processes.

2.1. The exploitation of the pressure solubility

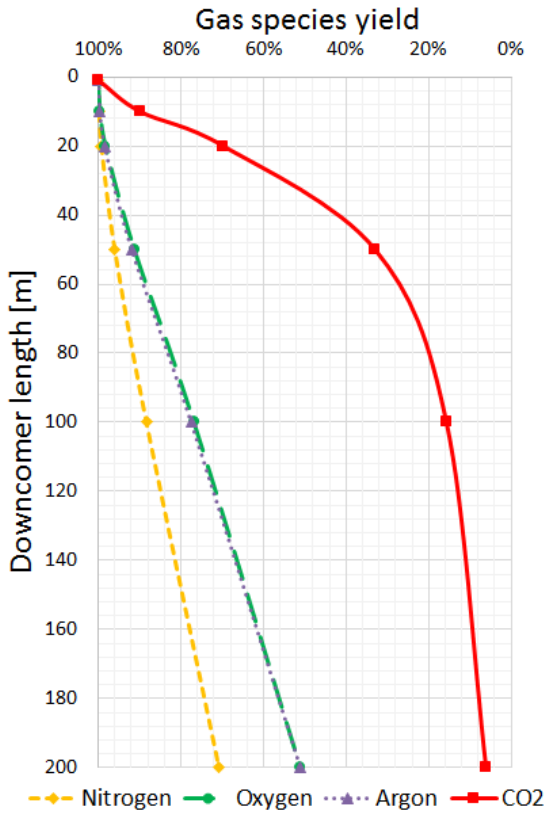

Fig. 1. Variation of air gas species yield with pressure, including coupled hydrodynamic, psychrometric and solubility kinetic effects.

By analysing the performance of historical hydraulic air compressors, the formerly underappreciated role of air species solubility in water has been revealed [1, 2]. Direct contact between air and water permits a portion of the gas being compressed to dissolve in the compressing liquid. More gas dissolves as the pressure increases. For typical HAC operating conditions (maximum 8.3 bar gauge, corresponding to a riser depth of ~80 metres – see [17] for a survey), this effect is governed by Henry's law [18], and equally applies to the CO_2 capture process considered herein. The solubility, or equilibrium concentration, of a gas species is evaluated as the product of the gas partial pressure and the species' Henry's constant. In Fig. 1, the effect of his relationship is derived for infinite media in contact. The interest in the application of HAC technology for carbon capture vests in the greater effect that the increase of pressure has on the solubility of the CO_2 in comparison to that of N_2, O_2 and Ar. It has now been predicted that the dissolution of mixture gas species is reduced by the absorption kinetics and hydro-dynamics in a HAC downcomer, rate limited at the liquid-gas interface across bubbles [19], although this awaits experimental verification. Figure 1 reports the variation of atmospheric gases' yield in the gaseous phase for increasing length of the downcomer. The results include the effect of the absorption kinetics as modelled by Young [19] and are obtained for a downcomer mass flow ratio of 1000 ($\dot{m}_W / \dot{m}_G = 1000$). The gas species yield represents the proportion of gas retained in the outlet gas stream at high pressure. For flow at the end of an 80 m long downcomer, over 80% of the CO_2 is dissolved in the water phase whereas only 10% of the N_2 dissolves. These dissolved gases pass to the riser through the physical gas-water separation process and evolve in the riser where the pressure reduces back to atmospheric and an enriched CO_2 gas stream results.

For increasing values of mass flow rate ratio, the amounts of each gas species that dissolve increase, due to the greater solubility potential. Physical gas-liquid separation devices that prolong contact between the two phases diminish the effects of diffusion rate limited solution kinetics and permit the two phases to approach equilibrium solubility concentrations. Adopting a separation gallery as presented in [3], rather than a cyclone separator, would achieve this. The design of a novel CO_2 capture system based on the HAC operating principle can be accomplished by directly exploiting the solubility phenomena characterizing the compression process.

2.2. Simulation of a two-stage HGC

As first suggested by Millar [1], a fossil fuelled power station can be coupled to a HGC by directing the exhaust gas stream to the mixing head of the compressor. The exhaust gas from a power plant principally constitutes CO_2, water vapour and N_2 with lesser proportions of unburned hydrocarbons or O_2, if the plant operates with significant air excess, and trace NO_x and SO_x.

Considering a stream of flue gas constituted by CO_2, H_2O, and N_2, as the combustion gas bubbles come into contact with the water in the downcomer shaft, one may expect the water vapour to condense into the water (if the combustion plant is not itself provided with a heat recovery system to condense the water vapour), and the remaining gases to dissolve into the liquid phase as the pressure increases in the downward shaft. At high pressure, most of the CO_2 will be dissolved in the water and the separation of the gas phase from the water will produce a gas stream principally constituting high pressure, dry, cool, N_2. which, independently, is of high economic value as an inert coolant or for pneumatic power. At this point the CO_2 is captured as a solute of the liquid phase water. The water depressurizes as it ascends the riser shaft and the solubility of gas species reduces toward the initial values at the common inlet and outlet pressures. This causes the gas phase dissolved in the liquid to come out of solution as the pressure returns to atmospheric. At the top of the riser a second gas-liquid separation device can be used to separate the liquid water phase and the gas phase. The collected gas phase has much higher concentration of CO_2 in comparison to the inlet stream but its purity is affected by the concurrent evolution of the N_2 from the liquid. A second stage of compression can be introduced to increase the purity of the CO_2-rich stream. Depending on the pressure reached by the second compression stage both the purity of the nitrogen and carbon dioxide stream can be improved.

The schematic in Fig. 2 presents the simulated two-stage HGC. The system comprises a natural gas CCGT plant with its exhaust connected to the first stage of HGC compression, which represent the main separation step. The second stage of compression, or purification stage, produces a rich stream of CO_2. This may be recompressed to a transportation and storage pressure of 150 bar, for example, in a seven stage conventional centrifugal compressor (7SCC).

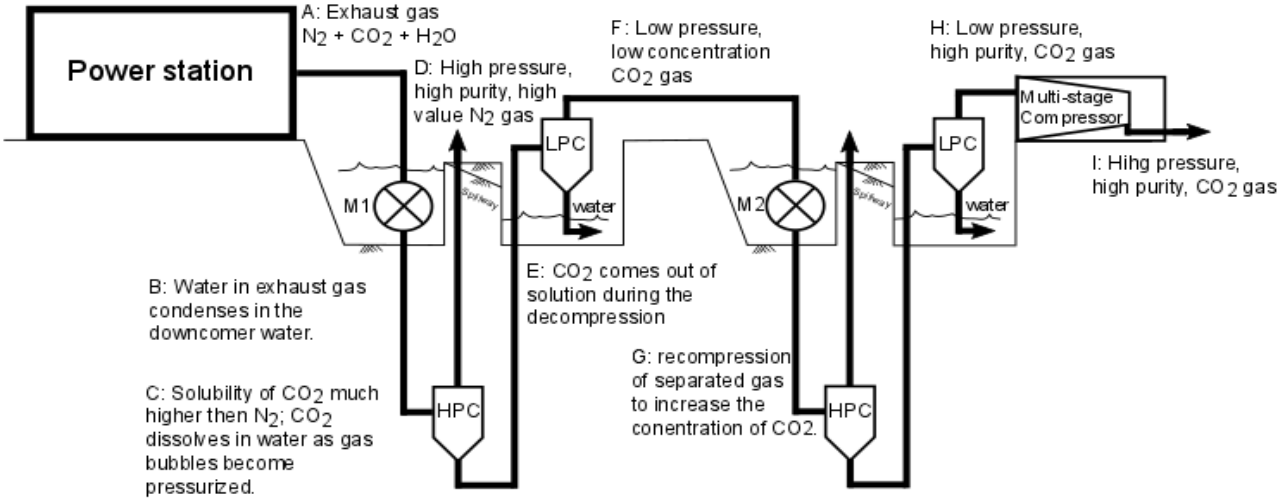

Fig. 2. Schematic of a two-stage hydraulic gas compressor for carbon capture application.

The first HGC (HGC1) has been defined with a similar configuration to that of the historical installation of Ragged Chutes (Cobalt, Ontario, Canada) [20]. The run-of-river HGC1 comprises a single 110 m deep downcomer shaft and a 94 m deep riser shaft, both of 4.5 m in diameter. The inlet water and gas mass flow rate can be established by balancing the inlet and outlet pressure to atmospheric boundary values and accounting for the pressure drop in the circuit. The resulting water flow rate is 37.6 tonne/s and the gas flow rate as it enters the mixing head is 25.6 kg/s. The latter represents the flue gas flow rate calculated for a 40 MW CCGT with an overall efficiency of 45% and an assumption of stoichiometric combustion of natural gas with high heating value of 55 MJ/kg.

The second HGC (HGC2) comprises a single 60 m deep downcomer and a 45 m deep riser shaft, with diameter of 3 m. The mass flow rates for HGC2 are 11.35 kg/s and 12.9 tonne/s for gas and water respectively; the mass flow rate ratio is 1133. The liquid-gas separations are performed in large cylindrical vessels 10 m high and 20 m wide, to increase the contact between the two phases and facilitate the achievement of the equilibrium solubility.

The results of solubility calculations for the HGC processes, assuming equilibrium solubility, are summarised in the process flow diagram of Fig. 3. 100% of the CO_2 entering the HGC1 is separated from the inlet gas stream. 14.1 kg/s N_2 at 10.2 bar, with 97.5 % (m/m) purity is also produced. The evolution of the gas from the liquid, taking place in the HGC1 riser shaft, produces an 11.4 kg/s gas stream comprising 38.7% (m/m) CO_2, a concentration that can be increased in HGC2. The products of HGC2 are 6.3 kg/s stream that is 90.6% (m/m) N_2, at 5.4 bar at the HPC and a 5.2 kg/s, 77.8% (m/m) CO_2 stream at atmospheric pressure at the low pressure cyclone (LPC).

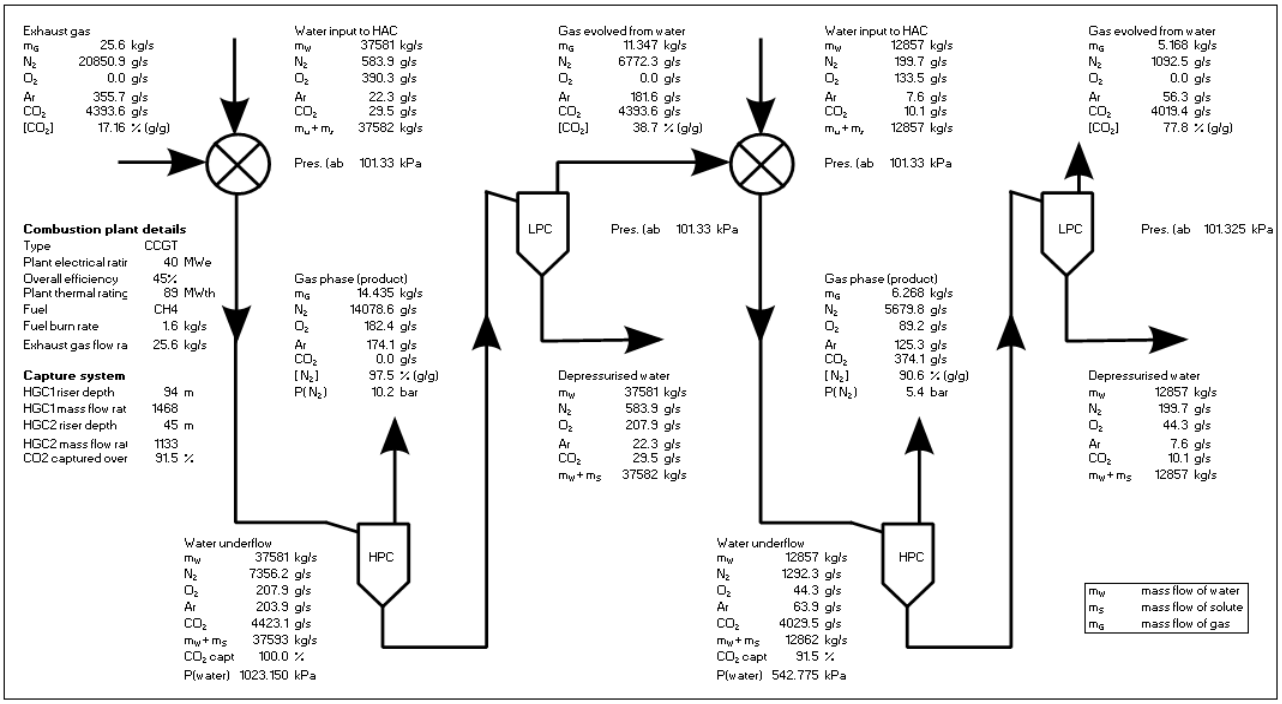

Fig. 3. Process flow diagram of the HGC1 and HGC2 cascade system.

For the illustrative case presented, 91.5% of the CO_2 presented at input to HGC1 is captured at the LPC of HGC2. Manipulation of the water mass flow rates, driving head as well as downcomer, HPC and LPC geometries, permit optimization of CO_2 recovery and purity metrics.

3. Techno-economic analysis

3.1. Outline of methodology

A techno-economic analysis of the system under development is required to assess its competitiveness with respect other post-combustion capture technologies.

The system evaluated in the analysis comprises:

- The two HGC cascade (HGC1 and HGC2) of Fig. 3.
- A 7 stage centrifugal compressor (7SCC) to recompress the CO_2 to 150 bar.

To obtain the input data for the economical assessment, 4 steps are performed:

1. Establish the flow rate and composition of the flue gas entering the capture system using data reported in the literature, or by means of a combustion analysis. With the assumption of stoichiometric combustion the flue gas flow rate determined for a 40 MW CCGT resulted 25.60 kg/s with 20.85 kg/s of N_2, 4.39 kg/s of CO_2 and 0.36 kg/s of Ar.
2. Simulate the mass and energy flows of HGC CO_2 capture cascade together with a CO_2 recompression process to reservoir (150 bar) pressure (for sequestration). For recompression, a 7 stage centrifugal compressor is assumed where each stage has an isentropic efficiency of 80% and inter- and after-cooling is complete between stages and electric motor efficiency of 95%.

3. Estimate the capital, operating and maintenance costs of the carbon dioxide separation and recompression system. Table A.1 in Appendix A reports the costs assumed for the components of the capture and recompression unit in detail. Operating and maintenance costs are presented in Table 2.
4. Follow accepted methodologies for calculation of the cost of CO_2 capture i): considering the HGC capture plant individually, and ii) considering the coupling of the capture plant with a CCGT, to establish the levelized cost of electricity (LCOE) with, and without, the capture system. Tables 2 and 3 report the results of the calculation for both options.

3.2. Cost metrics

Accepted economical assessment methodologies [22-24] for carbon capture systems evaluate two main parameters: the cost of CO_2 captured (related to the particular capture technology and plant type) and cost of CO_2 avoided (which compares the plant with capture to a "reference plant" without capture, and quantifies the average cost of avoiding a ton of atmospheric CO_2 emission while still providing a unit of useful product). Definitions are presented hereafter are as reported in [22]

$$LCOE = \frac{(TCC)(FCF) + FOM}{(CF)(8766)(MW)} + VOM + (HR)(FC) \tag{1}$$

The levelized cost of electricity generation (LCOE) is expressed in $/MWh and derived from: the total capital cost (TCC) – USD, the fixed charge factor – fraction/y, the fixed operating and maintenance costs (FOM) – USD/y, the variable non-fuel O&M costs – USD/MWh, the net power plant heat rate – MJ/MWh, the unit fuel cost (FC) – USD/MJ, (CF) the plant capacity factor – fraction, the total hours in an average year (8766), the net plant capacity (MW).

The cost of CO_2 avoided expressed in USD/t CO_2 can then be evaluated as follows:

$$\text{Cost of } CO_2 \text{ avoided} = \frac{LCOE_{ccs} - LCOE_{ref}}{(tCO_2/MWh)_{ref} - (tCO_2/MWh)_{rccs}} \tag{2}$$

where the subscripts '*ccs*' and '*ref*' refer to plants with and without CCS, respectively. The mass of CO_2 emitted to the atmosphere is expressed in tonne / MWh, based on the net capacity of each plant.

The cost of CO_2 captured is also reported in USD/t CO_2 and defined as:

$$\text{Cost of } CO_2 \text{ captured} = \frac{LCOE_{cc} - LCOE_{ref}}{(tCO_2/MWh)_{captured}} \tag{3}$$

where the denominator is the total mass of CO_2 captured per net MWh for the plant with capture (equal to the CO_2 produced minus the emitted one). The term $LCOE_{cc}$ excludes the cost of CO_2 transport and storage (T&S).

When considering the integration of the capture system with a power plant the energy penalty or capture energy requirements can also be evaluated by means of the following equation [22]

$$\frac{\%more\_input}{MWh} = \frac{\frac{1}{\eta_{cc}} - \frac{1}{\eta_{ref}}}{\frac{1}{\eta_{cc}}} \cdot 100 \tag{4}$$

3.3. Economic analysis

Table 2. Capture and recompression cost evaluated for the HGC capture system individually

Details of costs	Unit	HGC1 and HGC2	7SCC
Capital cost	CAD	9,625,000 (*1)	3,600,000 (*2)
Balance of Plant	CAD	2,000,000	-
Installation cost	CAD	-	360,000 (*3)
Total capital cost	CAD	11,625,000	3,960,000
Asset life	years	50 (*4)	12 (*5)
Discount rate	%	10	10
Annuitized capital cost	CAD/y	1,172,488	581,183
Motor rating	kW	0 (*6)	3,134
Operating hours	h/y	8,766 (*7)	8,766 (*7)
Electricity consumption	MWh/y	0	27,471
Electricity price	CAD/MWh	65 (*8)	65 (*8)
Annual electricity cost	CAD/y	0	1,785,625
Maintenance cost	% of capital cost per year	2	3.8
Maintenance cost	CAD/y	192,500	136,800
No. operatives		4	6
Labour	CAD/y	320,000 (*9)	480,000 (*9)
Total O&M costs	CAD/y	512,500	616,800
Total Electricity costs	CAD/y	0	1,785,625
Total Annual cost	CAD/y	1,684,988	2,983,608
Cost of CO_2 captured	**CAD/t**	**13.28**	**-**
Cost of CO_2 recompression	**CAD/t**		**23.5**
Total annual costs	CAD	4,668,596	
Annual CO_2 production	**tonnes**	**126,843**	
Cost of CO_2 captured and recompressed	**CAD/tonnes**	**36.8**	

Assumption
(*1) Estimated costs from construction contractor.
(*2) Estimated costs from Ingersoll Rand
(*3) Estimated as 10% of the installation cost of the compressor
(*4) Reliable and low maintenance facilities since the machinery has no, or few, moving parts
(*5) Estimated compressor lifetime
(*6) Run-of river HGCs configuration is assumed
(*7) Assuming a capacity factor of 100%
(*8) Assuming as reference industrial electricity prices typical of North Ontario as in [21]
(*9) Assumes operatives working shifts with an average salary of 80,000 CAD per year

For the run-of river system, the recompression process accounts for almost 2/3 of the total annuitized cost of CO_2 captured and recompression. As an extension, if a closed loop HGC configuration is assumed, in which the water is recirculated from the low pressure cyclone to the inlet reservoir by means of pumping, for the first stage of separation the cost of the capture process would increase to 46.1 CAD/t CO_2 while the total cost would reach 96.6 CAD/t CO_2. The pumps needed to recirculate the water flow rate would have a total installed capacity of 7304 kW (assuming a pump efficiency of 85% and a motor efficiency of 95%), causing the installation to become uncompetitive.

As reported in Table 3 the energy penalty for the simulated HGC capture system resulted of 8%. The energy intensity of the proposed system is appreciably lower than that characterizing the amine-absorption process, for which parasitic energy (the energy penalty) varies from 15 to 30% [25]. The

energy penalty of the HGC is evaluated for a run-of river configuration, thus no electricity is required to operate the HGCs. For a closed loop configuration additional energy would be required to recirculate the water in the circuit and the energy penalty would be increased accordingly. Considering the closed loop HGC1 described in Section 3.1 the energy penalty result as high as 26% due to the large water flow rate to be recirculated in the system. To obtain a competitive system with respect the amine-absorption, a run-of-river configuration of the system has to be employed. Alternatively, optimization manipulation of the mass flow ratio must be done to achieve reduced power required for the closed loop water recirculation.

Table 3. Performances and cost estimates for post-combustion capture at new NGCT power plant. The details of the cost and values assumed for the calculations are presented in Appendix B.

Plant performance measure		
Reference plant net power output	MW	40
Emission rate w/o capture	t CO_2/MWh	0.395
Emission rate with capture	t CO_2/MWh	0.037
Percent CO_2 reduction per MWh	%	91
Total CO_2 captured	Mt/y	0.13
Plant efficiency w/o capture, HHV basis	%	45
Plant efficiency w/ capture, HHV basis	%	41
Capture energy requirement	% more input/MWh	8
Plant cost measure		
Total capital reqm't. w/o capture	USD/kW	3,222
Total capital reqm't. with capture	USD/kW	3,893
Percent increase in capital cost for capture	%	21
LCOE w/o capture	USD/MWh	122
LCOE with capture	USD/MWh	140
Increase in LCOE with capture	USD/MWh	18
Percent increase in LCOE for capture	%	12.6
Cost of CO_2 captured	**USD/t CO_2**	**45**
Cost of CO_2 avoided, excl. T&S	**USD/t CO_2**	**49**

The results of the economical assessment, presented in Table 3, can be compared with those reported in the literature for state-of the art technologies as amine-based absorption. In particular Rubin et al. [22] reported a detailed review of the cost of CCS at natural gas combined cycle plants. With a reference plant net power output in the range 512 – 910 MW, the range of the cost of CO_2 captured is 48 – 111 USD/t CO_2, and that of the cost of CO_2 avoided, excluding transport and storage, is 58 – 121 USD/t CO_2.

The results obtained for the run-of-river HGCs capture appear promising in comparison to the literature values. However, three main improvements have to be considered to increase the fidelity and relevance of the analysis:

- Increase the scale of the system to couple the system with a large scale power plant with installed capacity of the order of 500 MW.
- Adopt a solubility model that includes the absorption kinetics in tandem with the hydrodynamics of the two phase flow as produced by Young.
- Achieve a level of purity of 90% in order to increase the economic value of the CO_2-rich stream produced.

To address the first improvement, a series of parallel HGC systems, identical to that analysed in section 2, can be proposed to obtain an overall process capable of handling a much larger volume of flue gas produced by the power plant. Capital costs will increase linearly with number of parallel streams, there are few economies of scale with this option.

Regarding the second aspect related to the absorption kinetics implementation, Young's non-equilibrium downcomer process model has been implemented to evaluate the difference in gas concentrations for the first separation stage of the capture system. For a downcomer of 4.5 m in diameter and 110 m length the difference between the concentrations (or equivalently the yields) determined using the equilibrium model and Young's model resulted in 9.5%, 7.6 % and 10.7% for N_2, CO_2 and Ar, respectively. An increased residence time of the gas phase in the high pressure separator would allow for a reduction of this difference. A larger plenum on the upper part of the separator would permits a prolonged storage of the high pressure gas and assist the process of evolution to equilibrium in solubility of the gas and liquid phase.

Further optimization so that the maximum potential for CO_2 dissolution is reached concurrently with the minimum potential for N_2 dissolution. The main parameter that permits the two conditions to be satisfied is the mass flow rate ratio, which also affects the gas flow rate entering the system. Three constrains have to be met when establishing the HGC configuration (i.e the mass ratio parameter) i) to grant the inlet of the total flow rate of exhaust gas from power plant ii) to permit the maximum dissolution of CO_2 during the compression and the separation stage iii) to minimize the dissolution of N_2 reducing the volume of water circulating into the system.

4. Exergy analysis of HGC CO_2 capture system

To produce a complete description of the carbon capture system exergy analysis can be applied to the three components required for the separation and recompression of the CO_2. Exergy analysis allows one to evaluate the thermodynamic value of the CO_2 captured and the pressurized N_2 gas streams. The exergetic content of a stream represents the maximum work that can be extracted from the flow of matter as it comes to equilibrium with a specified reference environment interacting only with the latter; it is a measure of the maximum capacity of a system to perform useful work as it proceeds to a specified final state in equilibrium with its surroundings [26, 27]. In formulating an exergy balance the lost work or irreversibility of the processes can be evaluated to assess the thermodynamic imperfections of the system.

For the open systems that characterized the HGC capture process, the exergy balance to be applied in steady state conditions equals the sum of the exergy of the thermal flow exchanged with a heat source at temperature T_i plus the mechanical-electric power, to the sum of the exergy content of each the mass flows entering or leaving the system and the flux of destroyed exergy (or rate of irreversibility):

$$\sum_{i=1}^{N} \dot{Q}_i \left(1 - \frac{T_0}{T_i} \right) + \dot{W} = \sum_{k=1}^{NC} \pm \dot{m}_k b + \dot{I} \quad , \tag{5}$$

where N is the total number of heat flows, NC is the number of streams crossing the system and T_0 is the temperature of the reference environment.

The exergy of a stream of substance crossing the system boundary is given by the sum of the kinetic, potential, physical and chemical exergy (excluding nuclear, magnetic, electrical and interfacial effects) [28]. The specific exergy of each mass flow is [29]:

$$b = \frac{v^2}{2} + gz + b_{ph} + b_{ch} \quad . \tag{6}$$

The physical exergy is calculated from the reference state (restricted dead state) at temperature T_0 and pressure p_0 without any change of the chemical composition of the considered substance. For a mixture of various gas species i, the physical exergy is obtained from:

$$b_{ph} = \sum x_i \left[h_i - h_{i,0} - T_0 \left(s_i - s_{i,0} \right) \right] . \tag{7}$$

The chemical exergy evaluates the chemical non-equilibrium of the system with respect the dead state (i.e. the conceptual environment within which the system is in thermal, mechanical and chemical equilibrium). The chemical exergy of a mixture of gas results from:

$$b_{ch} = \sum x_i \left[h_{i,0} - h_{i,00} - T_0 \left(s_{i,0} - s_{i,00} \right) \right]. \tag{8}$$

By applying the exergy balance, defined in (5), to each component of the HGC capture system, the rate of irreversibility produced by each part of the process can be established.

For the HGC1 and HGC2 the rate of irreversibility is establish as:

$$\dot{I} = \dot{m}_G b_{in,G} - y \cdot \dot{m}_G b_{out,G}^{HP} - (1-y) \cdot \dot{m}_G b_{out,G}^{LP} + \dot{m}_W (b_{in,W} - b_{out,W}), \tag{9}$$

where $b_{out,G}^{HP}$ is the outlet stream at high pressure, i.e. the N_2-rich stream while $b_{out,G}^{LP}$ is the outlet low pressure CO_2-rich stream.

For the 7SCC the rate of irreversibility is obtained as sum of the flux of exergy destroyed in each stage of compression and inter-refrigeration:

$$\dot{I} = \sum_{j=1}^{7} \dot{m}_G (b_{in,G}^{cj} - b_{out,G}^{cj}) - W_{el}^{\ j} + \dot{m}_G (b_{in,G}^{rj} - b_{out,G}^{rj}) \tag{10}$$

.

For all the three components it assumed that any heat developed during the processes is ultimately dissipated to the surrounding environment.

4.2. Results of exergy balance analysis

Table 4. Results of the exergy analysis of the HGC capture system

Specific exergy (kJ/kg)	*HGC1*	*HGC2*	Exergy (MW)	*HGC1*	*HGC2*
$b_{in,G}$	64.4	139.0	$B_{in,G}$	1.65	1.58
$b_{out,G}^{HP}$	222.1	172.0	$B_{out,G}^{HP}$	3.21	1.08
$b_{out,G}^{LP}$	139.3	309.7	$B_{out,G}^{HP}$	1.58	1.60
$b_{in,W}$	1.8	1.3	$B_{in,W}$	67.52	17.61
$b_{out,W}$	1.6	1.1	$B_{out,W}$	61.80	15.56

Table 5. Irreversibilities produced by the HGC capture system

	Rate of irreversibility (kW)	Percentage of the total irreversibility produced (%)
HGC1	2,579.9	57.9
HGC2	950.2	21.3
7SCC	926.0	20.8
Total	4,456.1	100

The results of the exergy analysis are reported in Table 4 and 5. The first stage of CO_2 separation accounts for the 58% of the irreversibilities created in the system, while those produced by the purification and recompression are comparable and represent around 21% each. The irreversibility of HGC1 is strongly affected by the high water mass flow rate: a small difference in specific exergy content, mostly due to reduction in potential energy between the inlet and outlet locations, results in a much higher variation of exergy content and total irreversibility produced. To reduce the flux of exergy destroyed, a reduction of the mass flow rate ratio could be suggested, but this will reduce the potential for gas dissolution (for both CO_2 and N_2) and so is a topic for further optimization study.

Discussion and conclusion

A techno-economic evaluation of a carbon capture system based on the HAC principle has been presented. Process flow calculations of a two-stage separation system have been presented to illustrate how, in the compression of the exhaust gas from a 40 MW CCGT, the preferential dissolution of the CO_2 into the liquid phase is exploited to achieve its separation. For a run-of river configuration of the capture system, the cost of CO_2 captured and avoided are promising but require experimental verification. Overall CO_2 capture and recompression cost is dominated by the capital and operating costs of a 7 stage centrifugal compressor to recompress the CO_2 after it has been separated from the exhaust gas stream by the HGC cascade. If an open or closed loop HGC system is considered, the annual costs of separation are higher due to the consumption of electricity to drive recirculating pumps, although this configuration potentially offers performance improvement (by reducing the mass flow rate ratio) through the addition of a 'salting-in' co-solute to the circulating water such as $Fe(OH)_3$ or intermediate concentrations of hydrochloric acid, perchloric acid, or nitric acid [30]. The use of some of these such co-solutes may present additional operating challenges, which have not, as yet, been explored.

The exergy evaluation of the capture system has indicated that the highest irreversibility is due to the HGC1 separation. High water flow rate promotes the irreversibility generated in HGC1 and increases the potential for N_2 dissolution. In turn, the purity of the final CO_2-rich steam is then reduced. The illustrated performance of the separation nevertheless may be assessed as 'promising' because the economic competitiveness of the run-of river HGC capture system has been illustrated. Optimization studies permit trade-offs between CO_2 purity, CO_2 recovery, energy consumed and exergetic irreversibility to be explored.

Acknowledgments

The authors wish to acknowledge the Ultra Deep Mine Network (UDMN), Ontario's Independent Electricity System Operator (IESO), the Northern Ontario Heritage Funding Corporation (NOHFC), MIRARCO Mining Innovation and Electrale Innovation Ltd for support for the Hydraulic Air Compressor Demonstrator Project (Project No. 3-004).

Appendix A

Table A.1. Details of the capital costs assumed for the economical assessment

HGC1	Cost (CAD)	Details
Blind sink shaft	1,950,000	Blind sink, 110 m deep, 4.5 m finished diameter, concrete lined, 5.7 m excavated diameter
Cyclone separator chamber (high P)	1,000,000	Cyclone separator chamber of dimensions 10 m in height and 20 m in diameter
Raise bore shaft	1,800,000	Blind sink, 94 m deep, 3.0 m finished diameter, concrete lined, 4.2 m excavated diameter
Cyclone separator chamber (low P)	1,000,000	As high pressure cyclone
Balance of plant	1,000,000	Including dam-reservoirs construction
Cooling pack	600,000	

Table A.1. (continued)

HGC2	Cost (CAD)	Details
Blind sink shaft	975,000	Blind sink, 60 m deep, 3.0 m finished diameter, concrete lined, 3.2 m excavated diameter
Cyclone separator chamber (high P)	1,000,000	Cyclone separator chamber of dimensions 10 m in height and 20 m in diameter
Raise bore shaft	900,000	Blind sink, 45 m deep, 3.0 m finished diameter, concrete lined, 4.2 m excavated diameter
Cyclone separator chamber (low P)	1,000,000	As high pressure cyclone
Balance of plant	1,000,000	Including dam-reservoirs construction
7SCC	Cost (CAD)	Details
Compressor	3,000,000	Price inquired for a Ingersoll Rand compressor

Appendix B

Table B.1. Details of the economical assessment based on the LCOE

Assumption and results			Notes
Reference plant			
Net plant capacity	40	MW	
Plant efficiency, HHV	45	%	
Plant capacity factor	100	%	
Annual production	350,640	MWh/y	
CO_2 emission flowrate	4.39	kg/s	
Plant emission	138,651	t/y	
Reference plant emission rate	0.395	tCO_2/MWh	
HHV	55.5	MJ/kg	
Inlet fuel mass flow rate	1.60	kg/s	
Energy consumed	2,805,120,000	MJ/y	
Fuel cost	6	USD/GJ	Average fuel cost [22]
Capital cost (660 MW)	1,050	USD/kW	Average capital cost for 660 MW plant [22]
Capital cost	3,222	USD/kW	Application of the 'six-tenth rule' to downscale the capital cost
Total capital cost	128,897,017	USD	
Discount rate	9	%	Average value [22]
Plant life	25		Average value [22]
Fixed charge factor	0.10	fraction/y	
Fixed O&M	12,889,702	USD/y	Assuming O&M costs equal to 10% of the total capital cost
Plant capacity factor	100	%	
Net plant capacity	40	MW	
Variable non fuel O&M	0	USD/MWh	
Net power plant heat rate	8,000	MJ/MWh	
unit fuel cost	0.006	USD/MJ	
Levelized cost of electricity generation	122	USD/MWh	

Table B.1. (continued)

Capture system			
Total capital cost for capture system	14,619,660	USD	Including the 7SCC replacement cost after 12 year of estimated life and assuming a conversion factor CAD to USD of 0.748
Fixed O&M capture system	844,716	USD/y	
Parasitic electricity	27,471	MWh/y	Due to 7SCC consumption
Energy requirement (energy penalty)	0.780	GJ/tCO_2	
Installed compressors capacity	3,134	kW	
Plant coupled with carbon capture system			
Net plant capacity	37	MW	
Net plant efficiency, HHV	41	%	
Plant capacity factor	100	%	
Annual production	323,169	MWh/y	
CO_2 capture efficiency	91.48	%	
CO_2 emission after capture	0.37	kg/s	
CO_2 captured per year	4.02	kg/s	
CO_2 emission after capture per year	11,809	t/y	
CO_2 captured per year	126,843	t/y	
Capture plant emission rate	0.037	tCO_2/MWh	
Capture plant rate of CO_2 captured	0.392	tCO_2/MWh	
HHV	55.5	MJ/kg	
Inlet fuel mass flow rate	1.60	kg/s	
Energy consumed	2,805,120,000	MJ/y	
Capture plant capital cost (TCR)	3,893	USD/kW	
Added TCR for capture	670	USD/kW	
% increase in capital cost	21		
Total capital cost	143,516,677	USD	
Discount rate	9	%	
Plant life	25		
Fixed charge factor	0.10	fraction/y	
Fixed O&M	13,734,418		
Plant capacity factor	100.00	%	
Net plant capacity	37	MW	
Variable non fuel O&M	0	USD/MWh	
Net power plant heat rate	8,680	MJ/MWh	
unit fuel cost	0.006	USD/MJ	
Levelized cost of electricity generation	140	USD/MWh	
Cost of CO_2 captured	45	USD/tCO_2	
Cost of CO_2 avoided, w/o T&S	49	USD/tCO_2	

Nomenclature

b specific exergy, J/kg
g acceleration of gravity, m/s2
h specific enthalpy, J/kg
HHV high heating value, MJ/kg
$\dot{I}$ rate of irreversibility, kW
$\dot{m}$ mass flow rate, kg/s
p pressure, kPa
$\dot{Q}$ heat transfer rate, kW
s specific entropy, J/kg
T temperature, °C
v velocity, m/s
W work, kJ
$\dot{W}$ rate of work, kW -
x mass fraction
y yield
z elevation

Greek symbols

η energy efficiency
ρ density, kg/m3

Subscripts and superscripts

00 dead state
0 restricted dead state
atm atmospheric
c compression
ch chemical
G gaseous phase
HP high pressure
i gas species
in inlet
LP low pressure
out outlet
ph physical
r inter-refrigeration
W liquid phase

References

[1] Millar DL., A review of the case for modern-day adoption of hydraulic air compressors. Appl Therm Eng 2014;69:55-77.

[2] Pavese V., Millar D., Verda V., Mechanical Efficiency of Hydraulic Air Compressors. ASME J Energy Resour Technol 2016;138(6):062005-062005-11.

[3] Pavese V., Energy and Exergy analysis of a Hydraulic Air Compressor for application in the mining industry [dissertation]. Torino, Italy: Politecnico di Torino; 2015.

[4] Rice W., Performance of Hydraulic Gas Compressor. ASME J Fluids Eng 1976;98:645-652.

[5] Plaza MG., Pevida C., Rubiera F., Ongoing Activity on CO_2 Capture in the Power Sector: Review of the Demonstration Projects Worldwide. In: Reference Module in Chemistry, Molecular Sciences and Chemical Engineering. Elsevier. 2016. p. 1-15. Available at: <http://dx.doi.org/10.1016/B978-0-12-409547-2.11129-1>

[6] Leung DYC., Caramanna G., Maroto-Valer MM., An overview of current status of carbon dioxide capture and storage technologies. Renew Sustain Energy Rev 2014;39:426-443.

[7] Yu CH., Huang CH., Tan CS, A review of CO2 capture by absorption and adsorption. Aerosol Air Qual Res 2012;12(5):745-769.

[8] Kenarsari SD., Yang D., Jiang G., Zhang S., Wang J., Russell AG., Wei Q., Fan M., Review of recent advances in carbon dioxide separation and capture. RSC Adv 2013;3(45):22739-22773.

[9] Spigarelli BP., Kawatra SK., Opportunities and challenges in carbon dioxide capture. J CO_2 Util 2013;1:69-87.

[10] Erans M., Manovic V., Anthony EJ., Calcium looping sorbents for CO_2 capture. Appl. Energy 2016;180:722-742.

[11] Abanades JC., Arias B., Lyngfelt A., Mattisson T., Wiley DE., Li H., Ho MT., Mangano E., Brandani S., Emerging CO_2 capture systems. Int J Greenh Gas Control 2015;40:126-166.

[12] Olajire AA., CO_2 capture and separation technologies for end-of-pipe applications–a review. Energy 2010;35(6):2610-2628.

[13] Shakerian F., Kim KH., Szulejko JE., Park JW., A comparative review between amines and ammonia as sorptive media for post-combustion CO_2 capture. Appl Energy 2015;148:10-22.

[14] Zaman M., Lee JH., Carbon capture from stationary power generation sources: A review of the current status of the technologies. Korean J Chem Eng 2013;30(8):1497-1526.

[15] Zhao M., Minett AI., Harris AT., A review of techno-economic models for the retrofitting of conventional pulverised-coal power plants for post-combustion capture (PCC) of CO_2. Energy Environ Sci 2012;6(1):25-40.

[16] Boot-Handford ME., Abanades JC., Anthony EJ., Blunt MJ., Brandani S., Dowell NM., Fernández JR., Ferrari MC., Gross R., Hallett JP., Haszeldine RS., Heptonstall P., Lyngfelt A., Makuch Z., Mangano E., Porter RTJ., Pourkashanian M., Rochelle GT., Shah N., Yao JG., Fennell PS., Carbon capture and storage update. Energy Environ Sci 2013;7(1):130-189.

[17] Langborne PL., Hydraulic Air Compression: Old Invention—New Energy Source. Chart Mech Eng 1979;26:76-81.

[18] Sander R., Compilation of Henry's law constants (version 4.0) for water as solvent. Atmos Chem Phys 2015;15(8):4399-4981.

[19] Young S., Pavese V., Hutchison A., Rico J., Millar DL., Interphase mass transfers in hydraulic air compressors for production of mine compressed air. In: Canello R., editor. ENERMIN 2016: Proceedings of the 3rd International Seminar on Energy Management in Mining; 2016 Aug 24-26; Santiago, Chile.

[20] Schulze LE., Hydraulic Air Compressor. Washington, D.C., USA: U.S. Department of the Interior, Bureau of Mines, Department of Energy; 1954. Information Circular No.: 7683.

[21] Ontario Energy Report, ONTARIO ENERGY REPORT Q2 2016 – Electricity. Available at: <https://www.ontarioenergyreport.ca/pdfs/5924_IESO_Q2OER2016_Electricity.pdf> .[accessed 19.5.2016].

[22] Rubin ES., Davison JE., Herzog HJ., The cost of CO_2 capture and storage. Int J Greenh Gas Control 2015;40:378-400.

[23] GCCSI, Strategic analysis of the global status of carbon capture and storage. Canberra ACT, Australia: Global CCS Institute, WorleyParsons; 2009 Nov. Report 5: synthesis report.

[24] IPCC, IPCC Special Report on Carbon Dioxide Capture and Storage. Cambridge, UK and New York, USA: Cambridge University Press, Intergovernmental Panel on Climate Change, Working Group III.

[25] Jassim MS., & Rochelle GT, Innovative absorber/stripper configurations for CO2 capture by aqueous monoethanolamine. Industrial & Engineering Chemistry Research 2006;45(8):2465-2472.

[26] Kotas T.J., The Exergy Method of Thermal Plant Analysis. London: Butterworths; 1985.

[27] Bejan A., Advanced Engineering Thermodynamics. New York: John Wiley & Sons; 1988.

[28] Szargut J., Morris D.R., Steward F.R., Exergy analysis of thermal, chemical and metallurgical processes. New York: Hemisphere Publ. Corp; 1988.

[29] Szargut J., Exergy method: technical and ecological applications. Southampton, Boston: WIT Press; 2005.

[30] Clever, H.L., An Evaluation of the Solubility of Carbon Dioxide in Aqueous Electrolyte Solutions. IUPAC-NIST Solubilities Database - NIST SDS 106, 1995. Available at: <http://srdata.nist.gov/solubility/sol_detail.aspx?goBack=Y&sysID=62_73> [accessed 15.9.16]